

Doping effect on the phase transition temperature in ferroelectric $\text{SrBi}_{2-x}\text{Nd}_x\text{Nb}_2\text{O}_9$ layer-structured ceramics: a micro-Raman scattering study

Kai Jiang, Wenwu Li, Xiangui Chen, Zhenni Zhan, Lin Sun, Zhigao Hu* and Junhao Chu

The temperature dependence of Raman spectra for $\text{SrBi}_{2-x}\text{Nd}_x\text{Nb}_2\text{O}_9$ ceramics (x from 0 to 0.2) has been studied in a wide temperature range from 80 to 873 K. It is found that the peak position of the $A_{1g}[\text{Nb}]$ phonon mode at 207 cm^{-1} , which is directly associated with the distortion of NbO_6 octahedron, decreases with increasing Nd composition, while the $A_{1g}[\text{O}]$ phonon mode at 835 cm^{-1} increases. Moreover, both the peak position and intensity of the $A_{1g}[\text{Nb}]$ phonon mode reveal strong anomalies around the ferroelectric to paraelectric phase transition temperature. It indicates that the phase transition temperature decreases from about 710 to 550 K with increasing Nd composition, which is due to the fact that the introduction of Nd ions in the Bi_2O_2 layers reduces the distortion extent of NbO_6 octahedron. Copyright © 2011 John Wiley & Sons, Ltd.

Keywords: $\text{SrBi}_{2-x}\text{Nd}_x\text{Nb}_2\text{O}_9$ ceramic; phase transition; Raman spectroscopy

Introduction

Bismuth layer structure ferroelectrics (BLSFs) have attracted considerable attention because of their potential application in ferroelectric random access memories, electro-optic switches, and other electronic devices.^[1–3] The general formula of BLSFs is given as $(\text{Bi}_2\text{O}_2)^{2+}(\text{A}_{m-1}\text{B}_m\text{O}_{3m+1})^{2-}$, where A and B are the two types of cations that enter the perovskite unit, and m is the number of perovskite unit cell between bismuth oxide layers.^[3–5] Especially, strontium barium niobate $\text{SrBi}_2\text{Nb}_2\text{O}_9$ (SBN), which is known to be an $m=2$ member of the BLSFs family, has been regarded as a promising ferroelectric material because of low dielectric constants and excellent fatigue resistance.^[5,6] It is well known that SBN crystallizes in the orthorhombic space group $A2_1am$ at room temperature (RT). At the temperature above the ferroelectric Curie temperature ($T_C \approx 705\text{ K}$), the structure of SBN belongs to the tetragonal paraelectric phase. The structure corresponds to $I4/mmm$ symmetry, which can result in 12 Raman-active modes: $4A_{1g} + 2B_{1g} + 6E_g$.^[7,8]

Recently, many research groups have focused on the doping effect on the fabrications and dielectric properties for SBN materials.^[2,3,9–12] The substitution of Ca ions in the Sr site for the SBN ceramic induced the increase in T_C , which is useful for the application in high-temperature resonators.^[11,12] However, the substitution of some rare earth ions such as La^{3+} or Pr^{3+} for Bi^{3+} in the Bi_2O_2 layers can result in a shift for the T_C to lower temperature.^[3,9,13] It is found that the behavior of the Nd-doped SBN ceramic tends to change from a normal ferroelectric to a relaxor type ferroelectric because of the introduction of Nd ions in the Bi_2O_2 layers.^[3,9,10,14] Up to now, a detailed understanding of the lattice dynamic properties and the phase transition behavior of Nd-doped SBN ceramics is still lacking. Raman spectroscopy is a

sensitive technique for investigating the structure modifications and lattice vibration modes, which can give the information on the changes of lattice vibrations and the occupying positions of doping ions. Thus, it is a powerful tool for the detection of phase transition in the doping-related ferroelectric materials.^[14–16]

In this paper, we have investigated the Nd doping effect on the Raman phonon modes and the phase transition from ferroelectric to paraelectric of $\text{SrBi}_{2-x}\text{Nd}_x\text{Nb}_2\text{O}_9$ (SBNN) ceramics by temperature-dependent Raman scattering. The Nd composition dependence of the phase transition temperature has been discussed in detail.

Experimental

The SBNN ($x=0, 0.05, 0.1, \text{ and } 0.2$) ceramics were prepared by a conventional solid-state reaction route, and SrCO_3 , Bi_2O_3 , Nb_2O_5 , and Nd_2O_3 were used as the starting materials. Details of the fabrication process for the ceramics can be found elsewhere.^[6,10] The X-ray diffraction analysis at RT indicates that the SBNN ceramics are of orthorhombic phase.^[6] Raman scattering experiments were carried out using a Jobin–Yvon LabRAM HR 800 UV micro-Raman spectrometer, excited by a 632.8 nm He–Ne laser with a spectral resolution of 0.65 cm^{-1} . Temperature-dependent measurements from 80 to 873 K were performed using the Linkam THMSE 600 heating stage, and the set-point stability is of better than 0.5 K.

* Correspondence to: Zhigao Hu, Key Laboratory of Polar Materials and Devices, Ministry of Education, Department of Electronic Engineering, East China Normal University, Shanghai 200241, China E-mail: zghu@ee.ecnu.edu.cn

Key Laboratory of Polar Materials and Devices, Ministry of Education Department of Electronic Engineering, East China Normal University Shanghai 200241, China

Results and Discussion

Figure 1(a) shows the Raman spectra of the SBNN ceramics with different Nd compositions at 80 K in the spectral range of 50–950 cm^{-1} . The scatter circle points are the experimental data and the solid lines are the fitting curves according to the Lorentzian multiplex fitting. The Raman selection rules allow 18 phonon modes ($4A_{1g} + 2B_{1g} + 6B_{2g} + 6B_{3g}$) for the SBN ceramics at low temperature.^[8] However, less than 12 phonon modes are observed because of the possible overlapping of the same symmetry vibration or the weak feature of some vibration bands.^[17] According to the assignment of $\text{SrBi}_2\text{Nb}_2\text{O}_9$ single crystal,^[8] the Raman phonon modes at about 61, 207, and 835 cm^{-1} can be assigned to the A_{1g} phonon mode, the vibrations at about 179 and 579 cm^{-1} can be assigned to the E_g phonon mode. However, the assignments of other phonon modes are still not clear. The internal vibrations of NbO_6 octahedra occur in the high-wavenumber mode region above 200 cm^{-1} because the intragroup binding energy within the NbO_6 octahedra is much larger than the intergroup or crystal binding energy.^[11] The composition dependence of the Raman shift for two typical phonon modes is illustrated in Fig. 1(b). Note that the modes at 207 and 835 cm^{-1} do not shift in the same direction with increasing Nb substitution. The $A_{1g}[\text{Nb}]$ phonon mode at 207 cm^{-1} , which arises from the distortion of NbO_6 octahedra, generally decreases with the Nd composition. It indicates that the introduction of Nd ions in the Bi_2O_2 layers may reduce the degree of distortion of NbO_6 octahedra.^[10] However, the $A_{1g}[\text{O}]$ phonon mode at 835 cm^{-1} mode corresponding to the symmetric Nb–O stretching vibration, increases with the substitution of Nd ions for Bi ions. Because the Nd^{3+} ions incorporation into Bi_2O_2 layers induces the bond relaxation in this layer, the neighboring NbO_6 octahedra might shrink, resulting in a blueshift in the peak position of the $A_{1g}[\text{O}]$ phonon mode.^[2]

To further understand the influence of Nd^{3+} ion substitution in the Bi_2O_2 layers on the phase transition behavior for the SBNN ceramics, we present in Figs 2 and 3 the temperature dependence of the Raman spectra for all the SBNN ceramics in the

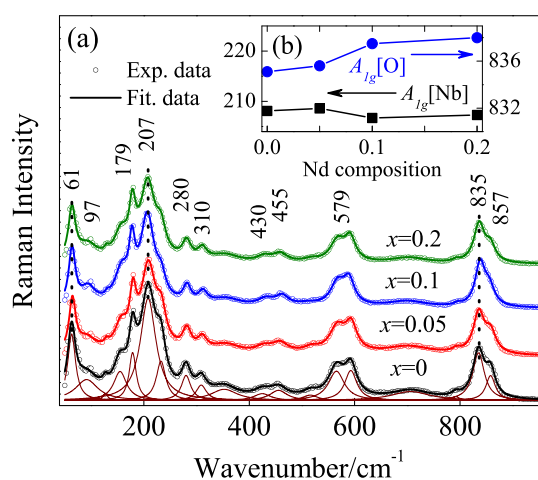


Figure 1. Raman scattering spectra of the SBNN ceramics with different Nd composition (x) recorded at 80 K. The scatter circle points are the experimental data and the solid lines are the fitting curves. The dashed lines clearly indicate some Raman-active phonon modes. The inset shows the peak wavenumber variation of the $A_{1g}[\text{Nb}]$ phonon mode at about 207 cm^{-1} and the $A_{1g}[\text{O}]$ phonon mode at about 835 cm^{-1} as a function of the Nd composition.

temperature range from 80 to 873 K. It is found that the $A_{1g}[\text{O}]$ phonon mode at about 835 cm^{-1} becomes broad and asymmetric, and there is no remarkable shift of this peak with the temperature. A strong broadening peak at about 579 cm^{-1} can be observed at 80 K because of the combined effects of two modes splitting from the E_g character mode. The broadening band can be assigned to a rigid sublattice mode, in which all the positive and negative ion displacements are equal and opposite.^[7] With increasing temperature, the peak position and intensity of the phonon mode present a decreasing trend. Because the mode is assigned to the asymmetric Nb–O vibration, it can be concluded that the NbO_6 octahedra is sensitive to the temperature. However, the $A_{1g}[\text{Bi}]$ phonon mode at about 60 cm^{-1} remains unchanged with increasing temperature, which indicates that the vibration of Bi ions in the Bi_2O_2 layers are not sensitive to the temperature. On the other hand, the phonon modes at about 280 and 310 cm^{-1} (labeled by *), which are associated with the O–Nb–O bending, become more difficult to be distinguished as the temperature increases and disappear at high temperature. Similar phenomena can be observed for the phonon modes in the range of 430–455 cm^{-1} (labeled by #). The band at about 455 cm^{-1} , which is ascribed to a Nb–O torsional mode, has been assigned as the E_g character and splits into two phonon modes centered at 430 and 455 cm^{-1} at lower temperature. As pointed out by Graves *et al.*,^[8] it can be ascribed to the fact that the several E_g phonon modes split into the B_{2g} and B_{3g} phonon modes during the tetragonal to orthorhombic transition. Moreover, the splitting of the phonon modes reveals the structural changes in the SBNN ceramics with the temperature.

In general, the phase transition in the BLSFs cannot be determined in terms of a single soft mode. They can be driven by various combinations for the displacive modes.^[18] It is clear that the $E_g[\text{Nb}]$ phonon mode at 179 cm^{-1} have a remarkable redshift with increasing temperature. A similar behavior of shifting to low wavenumber is also observed for the phonon mode at 97 cm^{-1} of the SBNN ceramics. In addition, the $E_g[\text{Nb}]$ and $A_{1g}[\text{Nb}]$ phonon modes are gradually overlapped with increasing temperature because of the disordered structure for the SBNN ceramics. The temperature dependence of the peak positions for the three Raman phonon modes (the $E_g[\text{Nb}]$, $A_{1g}[\text{Nb}]$ phonon modes and the mode at 97 cm^{-1}) is plotted in Fig. 4. The wavenumber of the $E_g[\text{Nb}]$ phonon mode decreases from 179 to 167 cm^{-1} when the temperature is changed from 80 to 873 K. The phonon mode at 97 cm^{-1} is shifted toward a lower wavenumber side of 8 cm^{-1} . The observed shifting of the peak position with the temperature can be ascribed to the effect of the thermal broadening and disorder: the anharmonic effects of the lattice. On the other hand, the change in bond length between the oxygen and cations can also induce the shifting.^[17] Note that an interesting temperature dependence of the wavenumber and intensity of the $A_{1g}[\text{Nb}]$ phonon mode was observed in this temperature region. The phonon mode originates from the distortion of vibration NbO_6 octahedra, which could reflect the distortion degree of NbO_6 octahedra. Thus, it can be expected that the $A_{1g}[\text{Nb}]$ phonon mode should be appropriate to probe the ferroelectric to paraelectric phase transition for the SBNN ceramics.

For all the SBNN ceramics, the peak position of the $A_{1g}[\text{Nb}]$ phonon mode decreases as the temperature is increased. However, an obviously anomalous behavior occurs beyond the phase transition temperatures: the wavenumber of this phonon mode sharply increases with increasing the temperature. Note that the temperature of the anomalous points is different for the four

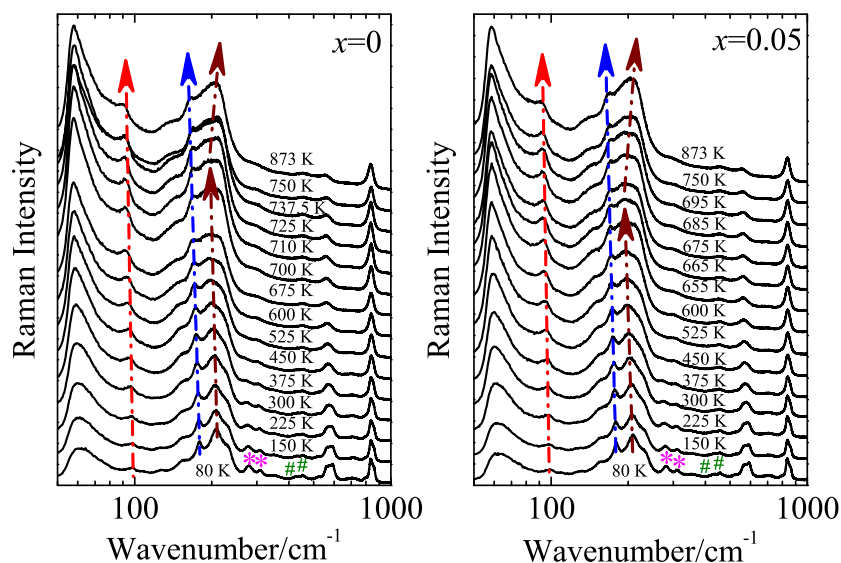


Figure 2. Temperature dependence of the Raman spectra for SBNN ceramics with the composition of $x = 0$ and 0.05 . The dashed arrows show the shift of the peak position of the phonon modes with the temperature. The symbol asterisk (*) and pound sign (#) indicate the two weak E_g phonon modes in the range of $280\text{--}310\text{ cm}^{-1}$ and $430\text{--}455\text{ cm}^{-1}$, respectively.

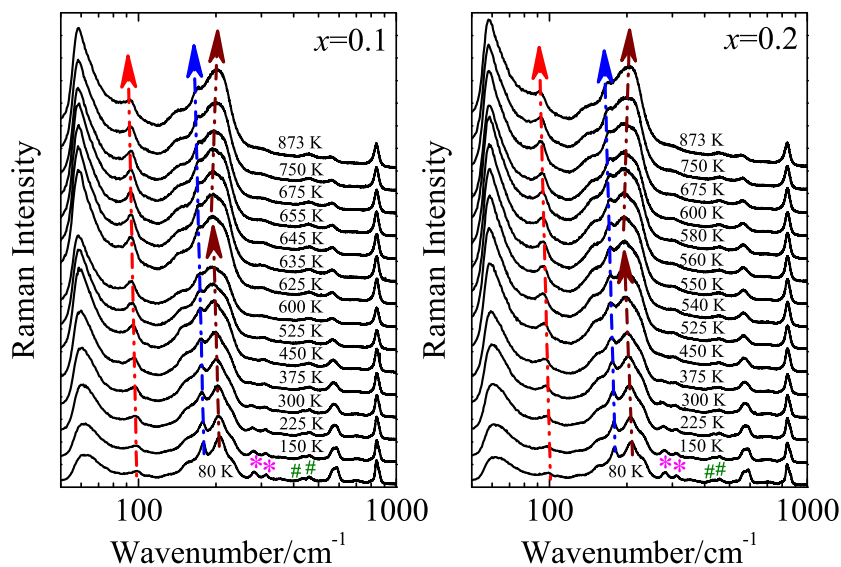


Figure 3. Temperature dependence of the Raman spectra for SBNN ceramics with the composition of $x = 0.1$ and 0.2 . Note that the symbols and arrows have the same meaning as those in Fig. 2.

ceramics: 710 K for $x = 0$, 665 K for $x = 0.05$, 625 K for $x = 0.1$ and 550 K for $x = 0.2$. The different anomalous points can be ascribed to the different Nd^{3+} incorporation in the Bi_2O_2 layers. The anomalous change in the $A_{1g}[\text{Nb}]$ phonon mode suggests that the phase transition from the orthorhombic to the tetragonal phase occurs at the temperature. The dashed lines in Fig. 4 shows the T_C for the four ceramics samples. It also indicates that the introduction of Nd leads to a decrease in the transition temperature.

Similar phenomena can be experimentally observed in the vicinity of the T_C when following the temperature evolution of the intensities for the three phonon modes in Figs 4(b), (d), (f), and (h). Generally, the intensities of the $A_{1g}[\text{Nb}]$ phonon mode for all the ceramics increase with the temperature. However, a sharp increase occurs as the temperature passes the T_C , which also indicates that there is the structural change in the SBNN

ceramics. The same behavior can be found in the intensities for the $E_g[\text{Nb}]$ phonon mode and the mode at 97 cm^{-1} . It is important to point out that the anomalous trends have been also reported for the ferroelectric to paraelectric phase transition of other ferroelectric materials (such as $\text{Bi}_{1-x}\text{Nd}_x\text{Ti}_3\text{O}_{12}$, LiCsSO_4 crystal, and BaTiO_3 nanotube arrays, etc.) using Raman scattering.^[17,19,20] A sharp change in the temperature dependence of both wavenumber and intensity of the $A_{1g}[\text{Nb}]$ phonon mode was applied to probe the phase transition of the SBNN ceramics.

The transition temperatures as a function of the Nd composition obtained from the Raman analysis are presented in Fig. 5. The T_C for the SBNN ceramics shifts to lower temperature with increasing Nd composition, and it can be well expressed by $(707\text{--}794.3x)\text{ K}$ with the solid line. The result demonstrates that the T_C decreases from about 710 to 550 K as the Nd composition

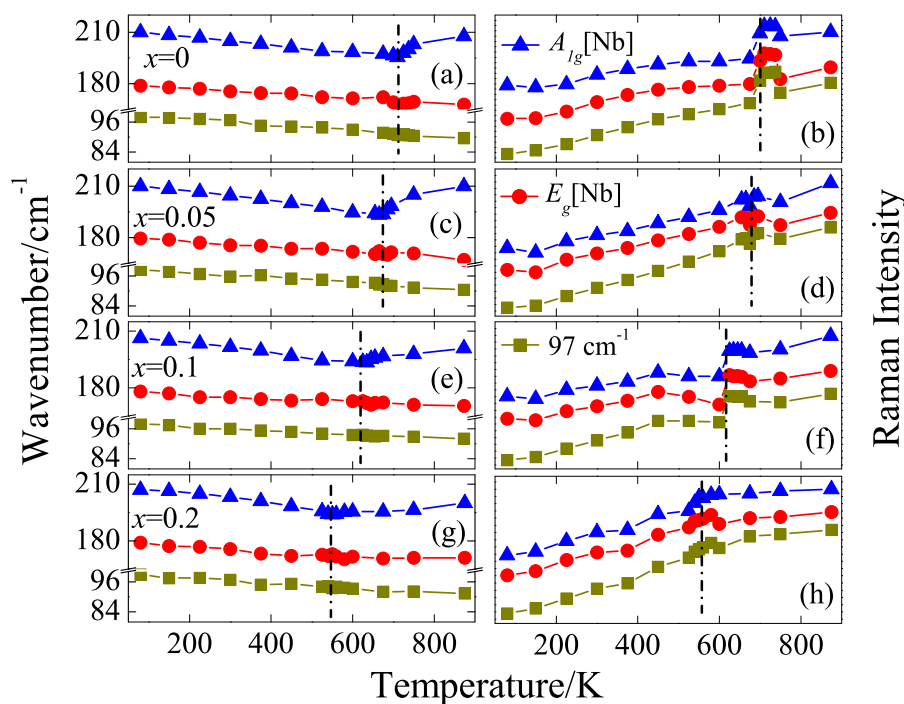


Figure 4. Raman shift and intensities of several Raman phonon modes (the $A_{1g}[\text{Nb}]$, $A_{1g}[\text{O}]$ and 97 cm^{-1} mode) as a function of the temperature for the SBNN ceramics. The dashed lines indicate that the anomalous behavior occurs in the vicinity of the ferroelectric to paraelectric phase transition temperatures.

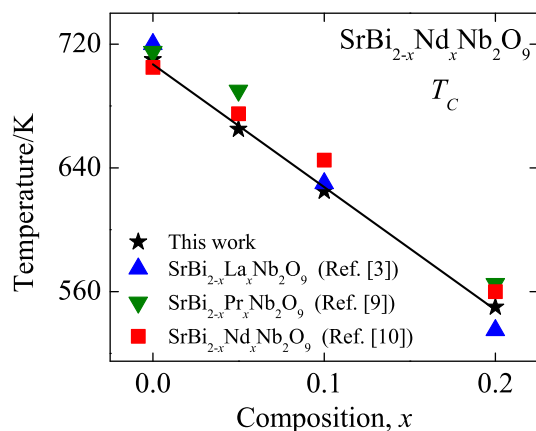


Figure 5. The Nd composition dependence of phase transition temperature in the SBNN ceramics as determined from the anomalous behaviors of several phonon modes in the Raman spectroscopy (★). For comparison, the variations of the T_C obtained by dielectric constant measurements for some rare earth ions doping in SBN (■, ▲, ▼) are also given. The solid line is the linearly fitting result to guide the eyes.

increases from 0 to 0.2. It indicates that the substitution of Nd ions for Bi^{3+} ions in the Bi_2O_2 layers results in the linear reduction of the T_C . The present work is in good agreement with the results from the dielectric spectroscopy.^[10] Compared with the effect on the transition temperature with the substitution of La^{3+} or Pr^{3+} for Bi^{3+} site, it can be concluded that the introduction of these rare ions in the Bi_2O_2 layers can induce a shift toward lower temperature for the T_C . This can be attributed to the substitution of these ions (having no lone pair electrons) at the bismuth site (having one lone pair of $6s^2$ electrons) resulting in the reduction in the distortion extent of NbO_6 octahedron. According to the

valence shell electron pair repulsion theory,^[10] the lone pair electrons tend to occupy more space than the bonding pair electrons. Thus, a significant redshift can be observed in the $A_{1g}[\text{Nb}]$ phonon mode of the SBNN ceramics with different Nd composition. In addition, the tilting angle of the NbO_6 octahedron obtained from $\text{Nb}-\text{O}-\text{Nb}$ bond angle, which could reflect the structure distortion degree of octahedron, decreases with increasing Nd composition.^[8] Furthermore, the tensile and compressive strain arising from the Bi_2O_2 layers and the perovskite-like layers in BLSFs, respectively, can also affect the structure of the NbO_6 octahedron. As a result, the substitution of the isovalent, larger, and nonpolarizable Nd^{3+} ions for the Bi^{3+} ions in Bi_2O_2 layers is expected to affect the bonding and hence the force constants among various ions. Therefore, there is a pronounced influence on the distortion of the NbO_6 octahedron, which results in the decrease of the transition temperature from the ferroelectric to the paraelectric state.

Conclusions

In summary, the composition dependence of phase transition temperature in the ferroelectric SBNN ceramics has been investigated using Raman spectroscopy in the temperature range from 80 to 873 K. It was found that a ferroelectric to paraelectric phase transition temperature decreases from 710 to 550 K with increasing Nd composition. The phase transition can be reflected by the critical changes in temperature dependence of wavenumber and intensity of the $A_{1g}[\text{Nb}]$ phonon mode. The decrease of the T_C can be attributed to the following reason: the reduced distortion extent and tilting angle of NbO_6 octahedron because of the Nd^{3+} incorporation into the Bi_2O_2 layers.

Acknowledgements

This work was financially supported by Natural Science Foundation of China (Grant Nos. 60906046 and 11074076), Major State Basic Research Development Program of China (Grant Nos. 2007CB924901 and 2011CB922200), Program of New Century Excellent Talents, MOE (Grant No. NCET-08-0192) and PCSIRT, Projects of Science and Technology Commission of Shanghai Municipality (Grant Nos. 10DJ1400201, 10SG28, 10ZR1409800, and 09ZZ42), and The Program for Professor of Special Appointment (Eastern Scholar) at Shanghai Institutions of Higher Learning.

References

- [1] Y. Shimakawa, H. Imai, H. Kimura, S. Kimura, Y. Kubo, E. Nishibori, M. Takata, M. Sakata, K. Kato, Z. Hiroi, *Phys. Rev. B* **2002**, *66*, 144110.
- [2] G. Z. Liu, C. Wang, H. S. Gu, H. B. Lu, *J. Phys. D: Appl. Phys.* **2007**, *40*, 7817.
- [3] P. Fang, H. Fan, J. Li, F. Liang, *J. Appl. Phys.* **2010**, *107*, 064104.
- [4] M. G. Stachiotti, C. O. Rodriguez, C. A. Draxl, N. E. Christensen, *Phys. Rev. B* **2000**, *61*, 14434.
- [5] D. P. Volanti, L. S. Cavalcante, E. C. Paris, A. Z. Simoes, D. Keyson, V. M. Longo, A. T. Figueiredo, E. Longo, J. A. Varela, F. S. D. Vicente, A. C. Hernandez, *Appl. Phys. Lett.* **2007**, *90*, 261913.
- [6] M. Zhu, L. Sun, W. W. Li, W. L. Yu, Y. W. Li, Z. G. Hu, J. H. Chu, *Mater. Res. Bull.* **2010**, *45*, 1654.
- [7] P. S. Dobal, R. S. Katiyar, *J. Raman Spectrosc.* **2002**, *33*, 405.
- [8] P. R. Graves, G. Hua, S. Myhra, J. G. Thompson, *J. Solid State Chem.* **1995**, *114*, 112.
- [9] S. M. Huang, C. D. Feng, L. D. Chen, X. W. Wen, *Solid State Commun.* **2005**, *133*, 375.
- [10] L. Sun, C. D. Feng, L. D. Chen, S. M. Huang, *J. Appl. Phys.* **2007**, *101*, 084102.
- [11] S. M. Huang, Y. C. Li, C. D. Feng, M. Gu, X. L. Liu, *J. Am. Ceram. Soc.* **2008**, *91*, 2933.
- [12] Y. Wu, M. J. Forbess, S. Seraji, S. J. Limmer, T. P. Chou, C. Nguyen, G. Cao, *J. Appl. Phys.* **2001**, *90*, 5296.
- [13] M. Verma, K. Sreenivas, V. Gupta, *J. Appl. Phys.* **2009**, *105*, 024511.
- [14] A. Speghini, M. Bettinelli, U. Caldiño, M. O. Ramírez, D. Jaque, L. E. Bausá, J. G. Solé, *J. Phys. D: Appl. Phys.* **2006**, *39*, 4930.
- [15] D. A. Tenne, A. Bruchhausen, N. D. L. Kimura, A. Fainstein, R. S. Katiyar, A. Cantarero, A. Soukiassian, V. Vaithyanathan, J. H. Haeni, W. Tian, D. G. Schlom, K. J. Choi, D. M. Kim, C. B. Eom, H. P. Sun, X. Q. Pan, Y. L. Li, L. Q. Chen, Q. X. Jia, S. M. Nakhmanson, K. M. Rabe, X. X. Xi, *Science* **2006**, *313*, 1614.
- [16] A. B. Shi, W. Z. Shen, H. Wu, *Appl. Phys. Lett.* **2007**, *91*, 112910.
- [17] K. Liang, Y. J. Qi, C. J. Lu, *J. Raman Spectrosc.* **2009**, *40*, 2088.
- [18] Y. E. Kitaev, M. I. Aroyo, J. M. P. Mato, *Phys. Rev. B* **2007**, *75*, 064110.
- [19] M. Kaczmarek, M. Wiesner, *J. Raman Spectrosc.* **2010**, *41*, 1765.
- [20] Y. Yang, X. H. Wang, C. K. Sun, L. T. Li, *J. Appl. Phys.* **2011**, *109*, 014109.